Macromolecules

pubs.acs.org/Macromolecules

Article

Are Well Performing Catalysts for the Ring Opening Polymerization of L-Lactide under Mild Laboratory Conditions Suitable for the Industrial Process? The Case of New Highly Active Zn(II) Catalysts

Massimo Christian D'Alterio, Ilaria D'Auria, Licia Gaeta, Consiglia Tedesco, Stefano Brenna, and Claudio Pellecchia*

Cite This: *Macromolecules* 2022, 55, 5115−5122

Read Online

ACCESS | Metrics & More | Article Recommendations | Supporting Information

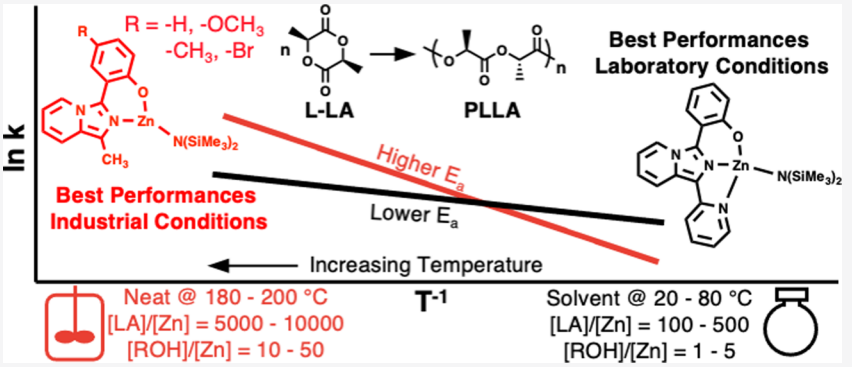

ABSTRACT: Poly(lactic acid) (PLA) is one of the best candidates as a sustainable plastic material for a circular economy, being biodegradable, bio-based, recyclable, and displaying good thermal and mechanical properties. The industrial production of PLA is mainly based on the ring opening polymerization (ROP) of L-lactide (L-LA) promoted by tin(II) 2-ethylhexanoate [$Sn(Oct)_2$] in a continuous solvent-free process operating at temperatures between 180 and 200 °C, above the melting point of the resulting isotactic polymer. Despite the huge efforts in the research of alternative catalysts based on less toxic metals, resulting in a plethora of highly active catalysts under laboratory mild conditions, very few candidates can compete with $Sn(Oct)_2$ under industrially relevant conditions. We report a family of new Zn(II) complexes, bearing variously substituted monoanionic [N,O$^-$] (imidazole[1,5-*a*]pyrid-3-yl)phenolate ligands, as catalysts for the ROP of L-LA under both mild (20 °C, solvent) and industrially relevant (190 °C, in the melt, technical grade unpurified monomer, very low catalyst loading) conditions. Interestingly, the best performing catalyst under mild conditions is the worst performing under harsh conditions, and, on the contrary, the less active catalysts under mild conditions compete well with $Sn(Oct)_2$ under industrially relevant conditions. Kinetic and DFT mechanistic investigations shed light on the non-trivial role of the 2-pyridine substituent in the catalytic performances at different temperatures. Preliminary depolymerization tests on commercial PLLA samples suggested that the new catalysts can also be a suitable candidate for the chemical recycling of PLA under mild conditions.

INTRODUCTION

Polylactic acid (PLA) is one of the few commercially available polymers assembling all the characteristics ideally necessary for an environmentally sustainable plastic material:[1] it is derived from biorenewable sources (such as corn, sugar cane, or even waste biomass),[2] it is biodegradable (although it degrades quickly only in industrial composting plants),[3] and it is well suited for a circular economy owing to the possibility of mechanical and chemical recycling.[4−6]

The current industrial production of PLA is in the order of 300,000 tons per year, which is expected to grow significantly in the coming years.[2] However, the growth potential of PLA-based materials for a variety of large-scale applications, currently dominated by polyolefins and poly(ethylene terephthalate), is subject to significant improvements in both the manufacturing process and the polymer properties. Industrially relevant targets for the expansion of PLA market are, for example, the increase of biodegradability in natural environments,[7] the reduction of the melt viscosity of high-molecular-weight PLLA for injection molding,[8] the production of PLA with higher impact resistance[9]

Received: April 8, 2022
Revised: May 24, 2022
Published: June 8, 2022

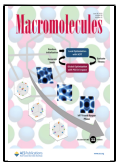

Scheme 1. Zn(II) Complexes of (Imidazo[1,5-*a*]pyrid-3-yl)phenol Ligands L1−L5

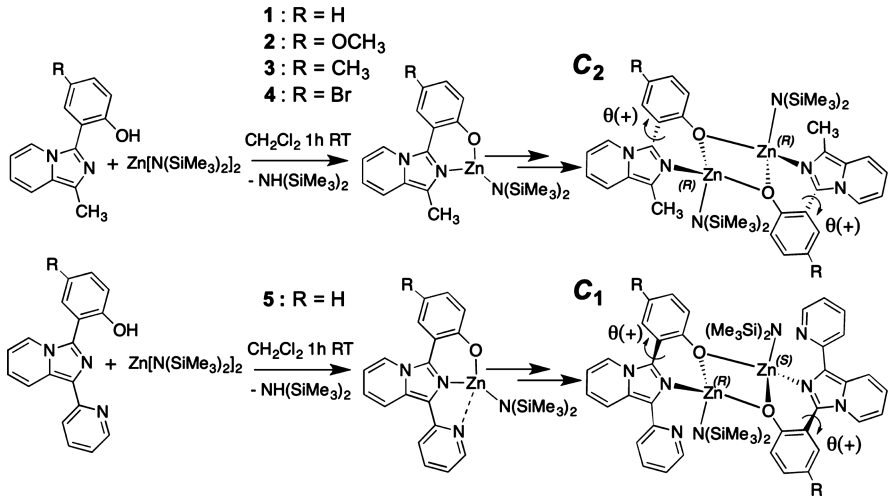

or elastomeric properties,[10] and, last but not least, the replacement of the catalytic system currently used in the industrial processes.[11] In fact, most of PLA industrial production is based on the ring opening polymerization (ROP) of L-lactide (L-LA), the (*S*,*S*) isomer of the dimeric lactone of lactic acid.[2] This synthetic strategy is promoted by initiators, typically metal-alkoxides, through a coordination−insertion mechanism, in which the lactide monomer, after coordination at the metal center, undergoes the ring opening by cleavage of the acyl group, followed by the insertion of the monomer into the metal−alkoxide bond. The pre-catalyst used in the industrial processes is Sn(II) 2-ethyl-hexanoate, commonly known as tin octanoate [$Sn(Oct)_2$], but the active species is believed to be a tin alkoxide generated in situ in the presence of excess of an alcohol.[12] $Sn(Oct)_2$ has a high catalytic activity under the process conditions ($T \geq 190°$ C, no solvent, LA/Sn mole ratios $\approx 10^4$) and allows good control of polymerization and the synthesis of high-molecular-weight polymers with minimal racemization problems when using an enantiopure monomer. However, the toxicity associated with tin residues in the polymer is a matter of concern, particularly for biomedical and food packaging applications. On this basis, catalysts based on non-toxic metals, such as magnesium, calcium, zinc, or aluminum, with ancillary ligands including alkoxides, β-diketiminates, bis(phenolates), Schiff bases, phenoxyimines, and so forth have been widely explored in the last 2 decades.[10,13−15] However, despite excellent performances, in many cases superior to that of $Sn(Oct)_2$, have been reported,[16] most studies were performed in conditions very far from those of the industrial process, that is, at room temperature in solvents such as methylene chloride or THF, or at slightly higher temperatures (50−80° C) in toluene, using recrystallized monomer at LA/catalyst molar ratios in a range of 100−1000.[10,17,18] Under these conditions, the most active catalysts quantitatively convert LA in a few minutes, with TOFs exceeding 10^4 h^{-1} and excellent control of the molecular weights and stereochemistry. Even when polymerization tests were reported in the absence of solvent, commonly used temperatures were in the range 130−150° C,[19,20] at which only the monomer, but not the isotactic PLLA, is above the melting temperature, a condition that would be impractical on an industrial scale for serious problems of viscosity of the reaction mixture and of diffusion of the monomer. Only a few catalysts active under conditions close to those of the industrial processes (T = 180−200 °C, technical grade monomer at L-LA/catalyst ratio 5000−10000:1, excess of alcohol) have been reported.[21,22]

In this paper, we report the synthesis and the characterization of a new family of Zn(II) complexes bearing variously substituted monoanionic [N,O$^-$] (Imidazole[1,5-*a*]pyrid-3-yl)phenolate ligands (**1**−**5**, see Scheme 1). Complexes **1**−**5** were tested as catalysts for the ROP of L-lactide (L-LA) both under mild (20 °C, solvent) and industrially relevant conditions (190 °C, neat), resulting in very promising performances. A thorough kinetic investigation showed that the best performing catalyst under mild conditions is the worst performing under harsh condition, and *vice versa*. A DFT mechanistic investigation provided a justification for the latter finding. More importantly, the new Zn complexes were compared with $Sn(Oct)_2$ under conditions similar to those of the industrial process, resulting in competitive performances. Finally, some preliminary results showed that these complexes also efficiently promote the methanolysis of commercial isotactic PLLA under mild conditions, affording methyl lactate with high selectivity, a potentially important further application in line with a circular economy approach.[5,6]

RESULTS AND DISCUSSION

Synthesis and Characterization of the Complexes. The (imidazole[1,5-*a*]pyrid-3-yl)phenol ligands L1−L5 and their homoleptic bis(chelate) Zn(II) complexes were previously reported.[23] Bidentate L1−L4 bear different electron-withdrawing or electron-donating substituents in the para position of the phenolic ring (−R), and a methyl group in the position 1 of the imidazopyridine ring, while L5 bears a H as R and a 2-pyridine moiety in the position 1 of the imidazopyridine ring, being a potentially tridentate ligand (Scheme 1). Following initial screening of the known homoleptic Zn(II) complexes in the ROP of L-LA, resulting in poor performances both in mild and harsh conditions (see Supporting Information, Table S1), we pursued the synthesis of heteroleptic complexes.

Complexes **1**−**5** were synthesized in almost quantitative yields by the reaction of equimolar amounts of L1−L5 and $Zn[(NSiMe_3)_2]_2$ in dichloromethane at 25 °C and recrystallized from toluene. The complexes were fully characterized by multinuclear NMR spectroscopy (Figures S1−S10) and high-resolution MALDI-ToF mass spectrometry (Figures S13−S22)

https://doi.org/10.1021/acs.macromol.2c00719
Macromolecules 2022, 55, 5115−5122

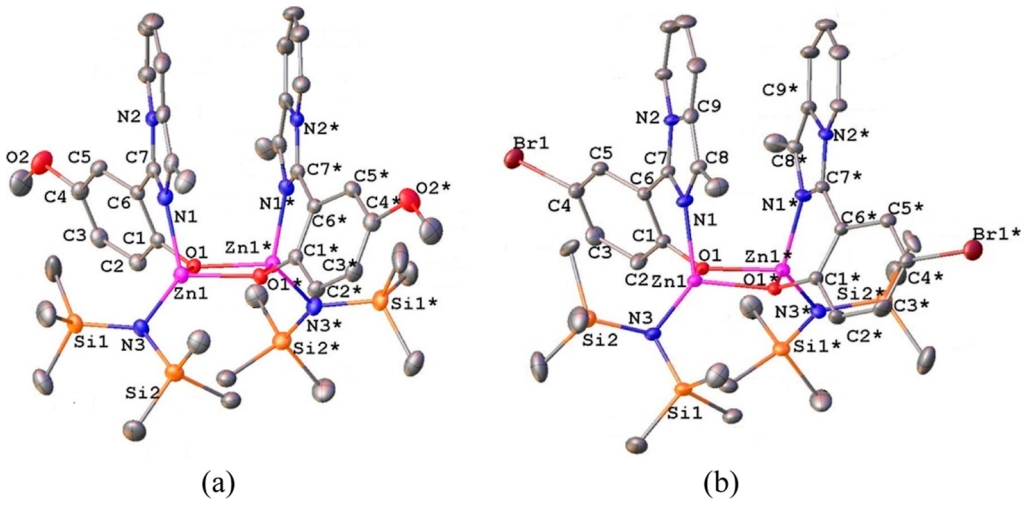

Figure 1. X-ray molecular structures (ORTEP) of complexes (a) **2** and (b) **4**. Ellipsoids are drawn at 20% probability level. Hydrogen atoms were omitted for clarity. * indicates a C_2 symmetry related atom.

Table 1. ROP of L-Lactide by 1−5 Under Variable Conditions

run	catalyst[a]	alcohol ($[ROH]_0/[Zn]_0$)	T [°C]	time [min]	Conv.[b] [%]	TOF ($[M]/[I])h^{-1}$	$M_{n,GPC}$[e] [kDa]	$M_{n,theo}$[f] [kDa]	M_w/M_n[e]
1[c]	**1**		20	30	2	3			
2[c]	**2**		20	30	2	3			
3[c]	**3**		20	30	2	3			
4[c]	**4**		20	30	2	3			
5[c]	**5**		20	30	20	80	18.6	5.8	1.8
6[c]	**1**	iPrOH (1)	20	30	65	260	13.3	18.7	1.1
7[c]	**2**	iPrOH (1)	20	30	70	280	12.8	20.1	1.1
8[c]	**3**	iPrOH (1)	20	30	75	302	15.6	21.6	1.1
9[c]	**4**	iPrOH (1)	20	30	56	224	9.7	16.1	1.2
10[c]	**5**	iPrOH (1)	20	30	80	320	17.5	23.0	1.2
11[d]	**1**	BnOH (5)	190	2	96	28800	19.4	27.6	1.4
12[d]	**2**	BnOH (5)	190	2	98	29400	16.1	28.0	1.7
13[d]	**3**	BnOH (5)	190	2	98	29400	18.5	28.0	1.6
14[d]	**4**	BnOH (5)	190	2	99	29700	16.8	28.4	1.5
15[d]	**5**	BnOH (5)	190	10	62	3720	8.1	17.8	1.2

[a]Catalyst = 10 μmol. [b]Conversion of monomer determined by ^{1}H NMR. [c]Polymerization conditions: $[LA]_0/[Zn]_0$ = 200, recrystallized L-LA; solvent = 2 mL of CH_2Cl_2. [d]Polymerization conditions: $[LA]_0/[Zn]_0$ = 1000, technical grade L-LA, no solvent. [e]Experimental M_n and M_w/M_n values determined by SEC in $CHCl_3$. [f]Calculated M_n of PLA (in g mol^{-1}) = 144.14 × ([LA]/[ROH]) × conversion of LA.

indicating the formation of heteroleptic dimeric species. Self-diffusion coefficients of complexes **1** and **5** were obtained from DOSY NMR experiments using the diffusion coefficient of TMSS as the internal reference standard. The estimated hydrodynamic volumes of the complexes are consistent with the formation of dimeric species (see the Supporting Information). The ^{1}H NMR and the ^{13}C NMR spectra of complexes **1**−**4** display 12 and 18 signals, respectively, as expected for C_2-symmetric dimeric species. On the contrary, 24 and 36 signals are detected in the ^{1}H NMR and the ^{13}C NMR spectra of complex **5**, in agreement with two asymmetrically wrapped ligands around two Zn centers. This feature made the punctual assignment of each atom of the ligand skeleton far less trivial than the highly symmetrical C_2 dimeric structures of **1**−**4**. Assignment of each resonance was possible by crossing the information coming from 1D and 2D homo- and heteronuclear NMR experiments. By following the scalar connectivity in the ^{1}H COSY (Figure S8), ^{13}C{^{1}H} HSQC, and ^{13}C{^{1}H} HMBC (Figure S9) NMR spectra, all ^{1}H and ^{13}C NMR resonances were assigned for each of the three aromatic rings in the two inequivalent [N,N,O] ligands (see the Supporting Information for full details). A comprehensive computational DFT analysis of all the possible dimeric species of complex **1**, chosen as the prototype for complexes **1**−**4**, and of complex **5** (see the Supporting Information), indicated that C_2 symmetric dimers with the two Zn centers in the same *R* or *S* configuration are the most stable for both the complexes (C_2-A of Scheme S1 and Table S1). Despite the high proximity of the -NSiMe$_3$ groups in this conformation, these structures are highly stabilized by the $\pi-\pi$ stacking interactions among the imidazopyridine moieties. This analysis well complies with the solution structures of complexes **1**−**4**, but it is not in agreement with the NMR spectra of complex **5**, indicating a C_1-symmetric structure (see above). Apparently, the 2-pyridine moiety increases the degrees of freedom and so the dimer is "freezed" in the most kinetically accessible among the thermodynamically feasible C_1 symmetric structures (C_1−C, C_1−F, or C_1−G, see Table S2 in the Supporting Information).

Orange prismatic single crystals of complexes **2** and **4** suitable for X-ray diffraction analysis were obtained by slowly cooling supersaturated toluene solutions. Crystal data and refinement

https://doi.org/10.1021/acs.macromol.2c00719
Macromolecules 2022, 55, 5115−5122

Table 2. Comparison of the Activities of Zn Catalyst 2 and $Sn(Oct)_2$ in the of ROP of L-LA at 190 °C and Low Catalyst Loadings[a]

run	catalyst	$[LA]_0/[Zn]_0$	$[ROH]_0/[Zn]_0$	T [°C]	Time [min]	Conv[b] [%]	TOF ($[M]/[I]h^{-1}$)	$M_{n,GPC}$[c] [kDa]	$M_{n,theo}$[d] [kDa]	M_w/M_n[c]
12	**2**	1000	5	190	2	98	29400	16.1	28.0	1.7
16	$Sn(Oct)_2$	1000	5	190	2	62	18600	14.7	17.8	1.0
17	**2**	2000	5	190	2.5	89	42720	29.8	51.2	1.4
18	$Sn(Oct)_2$	2000	5	190	2.5	85	40800	30.8	48.9	1.4
19	**2**	3000	10	190	3	93	55800	33.2	40.2	1.3
20[e]	**2**	3000	10	190	3	93	55800	28.1	40.2	1.3
21	$Sn(Oct)_2$	3000	10	190	3	88	52800	30.0	38.0	1.3
22	**2**	4000	15	190	3.5	92	63085	29.9	35.3	1.3
23	$Sn(Oct)_2$	4000	15	190	3.5	91	62400	28.6	34.9	1.3
24	**2**	5000	20	190	4	83	62250	24.6	29.9	1.3
25	$Sn(Oct)_2$	5000	20	190	4	93	69750	33.5	33.5	1.4

[a]Polymerization conditions: catalyst = 10 μmol, technical grade L-LA, no solvent, T = 190 °C. [b]Conversion of monomer determined by ^{1}H NMR. [c]Experimental M_n and M_w/M_n values determined by SEC in $CHCl_3$. [d]Calculated M_n of PLA (in g mol^{-1}) = 144.14 × ([LA]/[ROH]) × conversion of LA. [e]Run performed in air.

details are reported in the Supporting Information. Crystals of both **2** and **4** feature a monoclinic unit cell belonging to the centrosymmetric $C2/c$ space group. The X-ray molecular structures of complexes **2** and **4** (Figure 1) show similar structural features, both consisting of Zn dinuclear species, with the Zn atoms bridged by two phenolate oxygen atoms. Each zinc atom completes the coordination sphere bonding to the pyridine-like nitrogen of one imidazopyridine moiety and to one bis(trimethylsilyl)amido group. Bond lengths and angles for **2** and **4** are listed in Table S3. In both complexes, the crystallographic twofold axis (parallel to the b axis) passes through the center of mass of the Zn complex, being perpendicular to the complex equatorial plane, as defined by two zinc and two phenolate oxygen atoms. The two *bis*(trimethylsilyl)amido groups are located *cis* to each other. Interestingly, the imidazopyridine moieties are parallel to each other and oriented perpendicular to the complex equatorial plane with *anti*-located methyl groups, with distances in the range 3.5−3.7 Å. It is worth noting that the previously reported homoleptic dinuclear Zn complex bearing 2-(imidazo[1,5-*a*]pyridin-3-yl)phenolate ligands[24] does not display any intramolecular stacking interaction among the pyridine moieties because in that case, the coordination sphere of each Zn atom is saturated by two bidentate [N,O$^-$] ligands. For the related aminophenolate Zn(II) complexes reported by Jędrzkiewicz et al.,[25] where no stabilizing $\pi-\pi$ stacking interaction is possible, the repulsion among the $-NSiMe_3$ always drives the dimers to the C_i structures, where the two Zn centers bear an opposite configuration. The X-ray molecular structures of **2** and **4** perfectly fit within the C_2−A forecasted by the energetic DFT analysis.

ROP of L-Lactide. Complexes **1**−**5** were initially tested as catalysts for the ROP of L-LA under mild conditions, that is, at 20 °C in CH_2Cl_2 at L-LA/Zn ratio = 200 without any alcohol co-initiator: under these conditions, complexes **1**−**4** are hardly active, while **5** has a remarkably higher TOF (*cf.* runs 1−5, Table 1). Addition of 1 equiv of isopropanol as the co-initiator under otherwise identical conditions resulted in a significant increase of the TOF for all the complexes with a substantial reduction of the activity gap between **5** and **1**−**4**, although the former remains the most active under mild conditions (*cf.* runs 6−10, Table 1).

The high difference of activities between catalysts **1**−**4** and **5** in the absence of alcohol can be ascribed to the different stabilities of the more tightly bound C_2 symmetric dimers of **1**−**4** compared to the C_1 dimer of **5**, which is probably more easily broken in the presence of L-LA. Indeed, all the C_1 symmetric dimers calculated for complex **5** are 6−7 kcal/mol less stable than the C_2 symmetric one. Possibly, the alcoholysis reaction cleaves the dimeric structure of the precursors, generating more reactive Zn-OR species. NMR monitoring of the reaction of catalyst **2** with 3 equiv of L-LA in CD_2Cl_2 at 25 °C resulted in no significant spectral changes; then, 2 equiv of iPrOH was added to the solution and the ^{1}H NMR spectrum was recorded after 10 min, resulting in almost complete monomer consumption and in the appearance of the resonances of two new species, which were identified, also on the basis of a DOSY NMR experiment, as the homoleptic $(L2)_2Zn$ complex (probably the catalyst resting state, as already suggested for similar catalysts[25]) and the propagating active complex bearing the growing chain (see Figures S11 and S12).

The five catalysts were then tested in conditions closer to those of the industrial process (T = 190 °C, no solvent, L-LA/Zn molar ratio = 1000, 5 equiv of alcohol, technical grade unpurified monomer). Under these conditions, complexes **1**−**4** resulted very active, with TOF of the order of 3×10^4 h^{-1}, while **5** was much less active, with a TOF almost 1 order of magnitude lower (*cf.* runs 11−15, Table 1).

SEC analysis of the samples of Table 1 shows a significant difference between the experimental and the theoretical molecular weight for the sample prepared without alcohol (run 5), indicating a poor efficient initiation in the Zn−$NSi(Me_3)_2$, while a better agreement is found for samples prepared in the presence of alcohol.

The above preliminary screening suggests that the presence of a 2-pyridine in the position 1 of the imidazopyridine ring strongly affects the catalytic behavior of the catalysts, resulting in an opposite effect on the activity under mild and harsh conditions, respectively, while the electron-withdrawing or electron-donating substituents R are poorly effective. In order to verify if a different thermal stability of complexes **1**−**4** versus **5** would influence the catalytic performances, NMR spectra of **2** and **5** were recorded after heating the complexes at 190 °C in sealed vials, resulting in no spectral changes. A tentative rationalization of the substituent effects on the catalyst performances by a combined kinetic and DFT investigation is discussed in the following sections. The TOFs of complexes **1**−**4**, even using unpurified technical-grade monomer, are among the highest reported in the literature under industrially relevant conditions. For example, the homoleptic Zn complexes reported

https://doi.org/10.1021/acs.macromol.2c00719
Macromolecules 2022, 55, 5115−5122

by Jones and co-workers showed TOFs ranging between 11,400 and 54,000 h^{-1}.[21]

Therefore, a scale-up of the polymerization was carried out using complex **2** by gradually increasing both the monomer and the alcohol equivalents. In Table 2, the performances of catalyst **2** are compared with those of $Sn(Oct)_2$ under identical conditions, resulting in comparable or higher TOFs, thus demonstrating its uncommon resistance to protic impurities, alcohol excess, and high temperature. It is worth to note that the activity of **2** remains the same performing the polymerization either in an inert atmosphere (as usual) or in the presence of air (*cf.* runs 19 and 20). The polymer produced by **2** under these harsh conditions is highly isotactic, as shown by both homonuclear-decoupled ^1H NMR analysis and DSC analysis of the polymer sample obtained by run 22. The sample revealed a very low monomer racemization, identical to that of $Sn(Oct)_2$ under the same conditions (run 23) (see Figures S25 and S26). The highly regular microstructure of the polymer results in a high T_m [174.3 °C of the polymer sample obtained by **2** vs 173.9 °C of polymer sample obtained by $Sn(Oct)_2$, see Figures S27 and S28].

Two low-molecular-weight PLA samples were purposely prepared for MALDI-TOF MS analysis using catalyst **2** ([LA]/[BnOH]/[Zn] = 200:10:1) either in dichloromethane at 25 °C or in the melt at 190 °C. End group analysis indicated the presence of Ph−CH_2−O and CH(CH_3)−OH, confirming in both cases that ROP of L-LA is initiated by BnOH. Transesterification processes are absent at 25 °C, while they occur to a significant extent at 190 °C as generally observed (see Figures S23 and S24).

Kinetic Investigation. The kinetics of polymerization of L-LA were investigated at 20 and 50 °C in solution (in dichloromethane and toluene, respectively) for catalysts **1**−**5** using [Zn] = 5 mM, $[LA]_0/[Zn]_0 = 400$, and $[ROH]_0/[Zn]_0 = 1$ (ROH = benzyl alcohol). The kinetics of polymerization were also studied in the melt at 190 °C for **1**−**5** employing 1×10^{-5} mol of catalyst, $LA_0/Zn_0 = 1000$ (monomer was technical grade L-LA) and $[ROH]_0/[Zn]_0 = 1$. The detailed experimental procedure is reported in the Supporting Information. In all cases, the polymerization followed pseudo first-order kinetics in [L-LA], implying that the concentration of the active species remained unchanged during the run. The apparent propagation rate constants (k_{app}) were evaluated by pseudo-first-order kinetic plots of $\ln([L\text{-}LA]_0/[L\text{-}LA]_t)$ versus time (see Supporting Information, Figures S29−S34) and they are reported in Table 3 for catalysts **1**−**5**, and, for comparison, for $Sn(Oct)_2$ tested in the same conditions at 190 °C.

The values of the k_{app}'s reported in Table 3 for Zn catalysts **1**−**5** confirm that the most significant effect on the polymerization activity is played by the 2-pyridine substituent in the R′ position, while the influence of the R substituents is minor. In fact, **5** has the highest k_{app} in solution at 20 °C but, on the contrary, its k_{app} is 1 order of magnitude lower than those of catalysts **1**−**4** in the melt at 190 °C. It is worth to note that in these conditions at 190 °C, k_{app} values of **1**−**4** are around 2−3 times larger than k_{app} of $Sn(Oct)_2$.

To better understand the influence of the R′ substituent, we determined the k_{app}' values of **3** and **5** also at 65 and 80 °C (Table 3). As shown in Figure 2, by plotting ln k_p versus $1/T$ (where T is the temperature of the polymerization and k_p is obtained from the relationship $k_{app} = k_p[Zn]_0$), the activation energy of the polymerization for the two catalysts can be obtained according to the Arrhenius equation $\ln(k_p) = \ln(A) - \Delta E_a/RT$.

Table 3. Kinetic Rate Constants of L-LA Polymerization Promoted by 1−5 and $Sn(Oct)_2$ Under Different Conditions

catalyst	solvent	T [°C]	k_{app} [s^{-1}]
1	DCM	20	5.23×10^{-4}
2	DCM	20	5.31×10^{-4}
3	DCM	20	8.19×10^{-4}
4	DCM	20	5.13×10^{-4}
5	DCM	20	9.34×10^{-4}
1	toluene	50	1.95×10^{-3}
2	toluene	50	3.76×10^{-3}
3	toluene	50	3.54×10^{-3}
4	toluene	50	2.15×10^{-3}
5	toluene	50	2.09×10^{-3}
1	neat	190	7.19×10^{-2}
2	neat	190	5.53×10^{-2}
3	neat	190	4.66×10^{-2}
4	neat	190	5.77×10^{-2}
5	neat	190	4.13×10^{-3}
Sn(Oct)$_2$	neat	190	2.00×10^{-2}
3	toluene	65	8.20×10^{-3}
3	toluene	80	1.41×10^{-2}
5	toluene	65	4.45×10^{-3}
5	toluene	80	1.02×10^{-2}

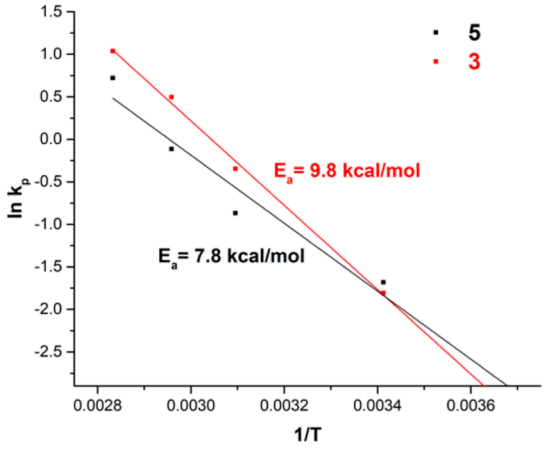

Figure 2. Arrhenius plots for **3** (red, R^2 = 0.997) and **5** (black, R^2 = 0.944).

The activation energies for **3** and **5** are, respectively, 9.8 and 7.8 kcal/mol. It is remarkable that just a subtle difference in activation energy places catalysts **1**−**4** as candidate substitutes of $Sn(Oct)_2$ under high temperature industrial conditions, whereas **5** remains appealing only in lab-scale applications for mild-condition reactions, a general warning for the large number of catalysts successfully tested under the latter conditions in the literature.

DFT Investigation. To shed light on the mechanistic details of the polymerization and on the origin of the difference of activity between **3** and **5**, we modeled the first insertion of the L-LA into the Zn−OR bond. We assumed that the alcoholysis of the Zn−N($SiMe_3$)$_2$ is a fast and quantitative reaction. To reduce the degrees of freedom, we substituted the initiating −O−CH_2−Ph with −OCH_3. In Scheme 2, we report the ROP cycle catalyzed by a Zn−OCH_3 catalyst. The ROP operates with a coordination−insertion mechanism in which the first transition

https://doi.org/10.1021/acs.macromol.2c00719
Macromolecules 2022, 55, 5115−5122

Scheme 2. Ring Opening Catalytic Cycle of L-LA Polymerization.

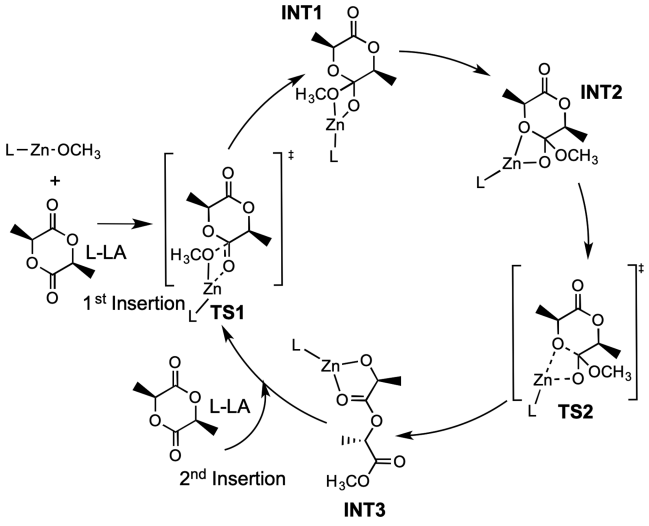

state (TS) for the nucleophilic addition (TS1) of the $-OCH_3$ is followed by a second TS for the ring opening of L-LA (TS2). Between these two TSs, at least two intermediates (INT1 and INT2) are present.[26,27] Once the L-LA ring is opened (INT3), another L-LA molecule can insert in the newly generated Zn−OR bond.

In Figure 3, we report the minimum energy path (MEP) for the first insertion of L-LA with the *re* enantioface in the Zn−OCH_3 bond for **3** (left) and **5** (right), respectively. Other mechanistic details are reported in the Supporting Information. The rate-limiting step for both these reactions is the nucleophilic attack (TS1) with an activation energy of, respectively, 9.4 kcal/mol for **3** and 6.2 kcal/mol for **5**. It is worth to note that if the MEP for 5 is calculated assuming bidentate ligand coordination (i.e., with a dangling pyridine moiety), the energetic barriers of **3** and **5** are comparable (respectively, 9.4 and 9.0 kcal/mol, see Figure S38 in the Supporting Information). Thus, the coordination of the 2-pyridine moiety lowers the activation energy of the reaction, in agreement with the experimental results, confirming the involvement of **5** as a tridentate ligand during the reaction. The theoretical results also fit well in terms of $\Delta\Delta G$ between the activation energy of **3** and **5** (2.0 kcal/mol experimental vs 3.2 kcal/mol theoretical). Finally, the RDSs TS1 were modeled also for catalysts 1, 2, and 4, resulting in activation energies of 9.2, 9.2, and 9.1 kcal/mol, respectively, thus confirming the experimental evidence that the modifications of R moieties are not influential.

Depolymerization of PLA via Methanolysis. As mentioned in the Introduction, chemical recycling of polymers has recently become a key target for the sustainability of plastics in a circular economy.[4,6] The controlled depolymerization of PLA through transesterification reactions with either methanol or ethanol affords methyl or ethyl lactate as valuable chemicals.[28−31] Thus, we have preliminary tested complex **5** for the depolymerization of a commercial sample of PLLA via methanolysis under the conditions reported by Jones et al.,[30] that is, using 1 mol % of Zn catalyst with respect to the number of ester linkages in either CH_2Cl_2 or THF solvent at 40 °C. The main reaction conditions and results are summarized in Table 4, while the details of the experimental procedure are reported in

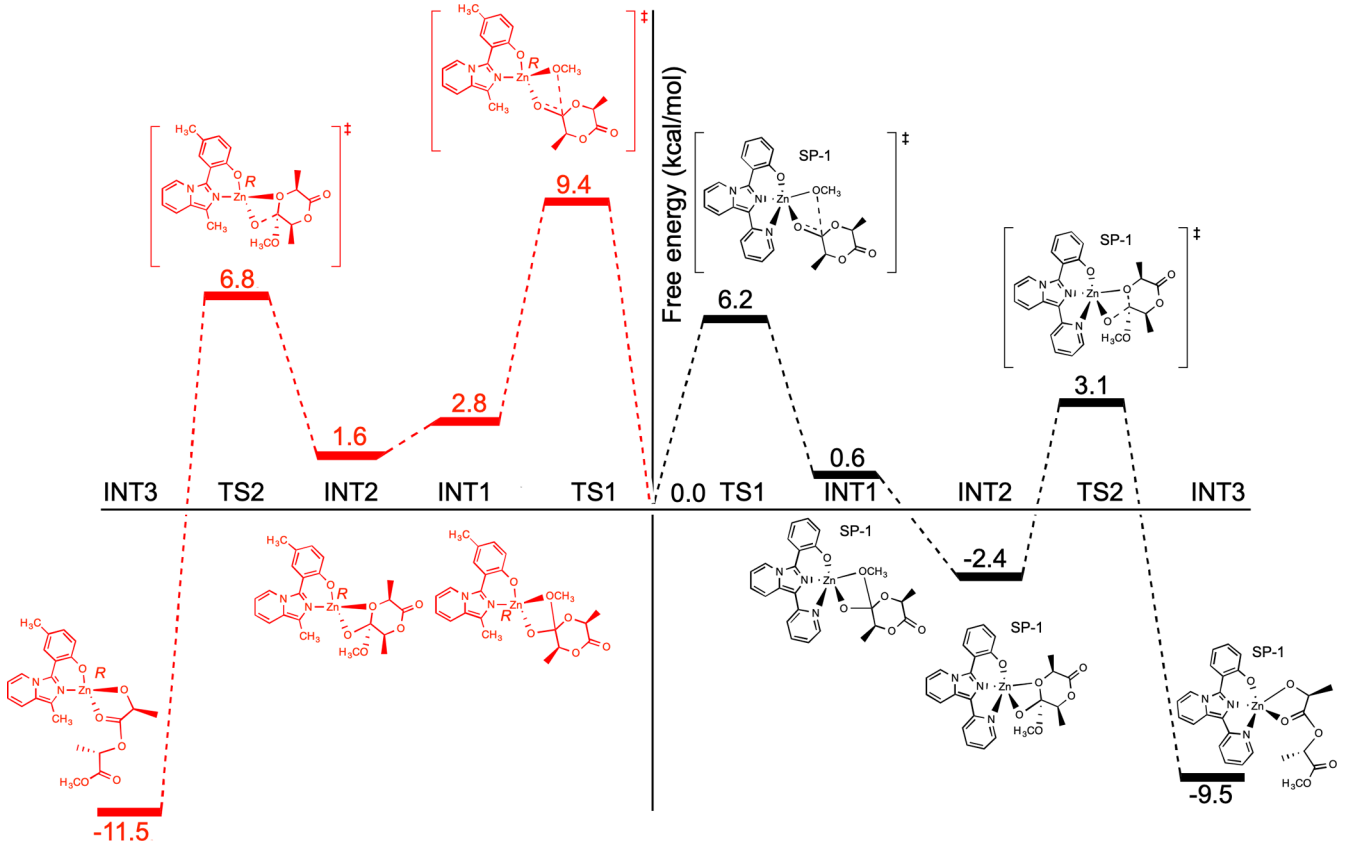

Figure 3. MEP for the first insertion of L-LA in the Zn−OCH_3 bond of **3** (left, in red) and **5** (right, black).

https://doi.org/10.1021/acs.macromol.2c00719
Macromolecules 2022, 55, 5115−5122

Table 4. Methanolysis of Commercial PLLA by Complex 5[a]

run	solvent	t [min]	X_{Int}[b] [%]	S_{Me-LA}[c] [%]	Y_{Me-LA}[d] [%]
25	DCM	5	38.3	10.3	3.94
26	DCM	10	65.6	26.0	17.1
27	DCM	15	86.6	42.6	36.9
28	DCM	20	93.1	55.2	51.4
29	DCM	25	98.4	60.1	59.2
30	DCM	30	99.1	62.8	62.2
31	THF	5	14.7	10.6	1.55
32	THF	10	38.1	14.4	5.48
33	THF	15	59.2	28.3	16.8
34	THF	20	71.7	34.7	24.9
35	THF	25	78.0	43.0	33.6
36	THF	30	83.0	49.4	41.1
37	THF	60	99.9	91.1	91.0
38	-[e]	60	88.6	100	88.6

[a]Reaction conditions: 0.25 g of PLLA (Sulzer L99L, M_n = 85 kDa, L-LA content = 99%), MeOH = 1 ml (n_{MeOH}/n_{ester} = 7:1), solvent = 4 mL, **5** = 35 μmol = 1 mol % relative to ester linkages, T = 40 °C, time = 1 h. [b]Conversion of internal methine groups; [c]selectivity in methyl lactate; [d]yield in methyl lactate; all the latter parameters were determined from ^{1}H NMR. [e]No solvent, 5 mL of CH_3OH at 65 °C.

the Supporting Information. According to the literature,[28−31] the methanolysis of PLA under these conditions proceeds via initial random cleavage of internal ester bonds leading to oligomers which are then converted into methyl lactate. Analysis of the methine region of the ^{1}H NMR spectrum allows the determination of the conversion of internal methines (X_{int}), the yield in methyl lactate (Y_{Me-La}), and the selectivity in methyl lactate (S_{Me-La}).

The preliminary results displayed in Table 4 show that **5** is highly active in the methanolysis of a high-molecular-weight commercial PLLA sample in both solvents: quantitative degradation was achieved in 30 min in CH_2Cl_2 and in 60 min in THF, in both cases with excellent selectivity toward methyl lactate. The apparent propagation rate constants (k_{app}) were evaluated by pseudo-first-order kinetic plots of $\ln([Int]_0/[Int]_t)$ versus time (where $[Int]_t$ is the fraction of unconverted internal methine carbons at time t, see the Supporting Information for further details). The calculated k_{app} for methanolysis is 2.5 × 10^{-3} s^{-1} in CH_2Cl_2 and 9.9 × 10^{-4} s^{-1} in THF, in both cases significantly larger than those reported in ref 30. Highly efficient degradation with 100% selectivity to methyl lactate was achieved in the absence of solvents using only boiling methanol at 65 °C for 1 h (see run 38, Table 4).

CONCLUSIONS

Five new heteroleptic Zn(II) complexes with (imidazole[1,5-*a*]pyrid-3-yl)phenolate ligands were synthesized and tested in the ROP of L-LA: the polymerization results showed that the trend in the performances of the catalysts are very different using either typical mild laboratory conditions (i.e., room temperature, dissolving the purified monomer in methylene chloride, and using low monomer/catalyst ratios) or industrially relevant conditions (i.e., technical-grade monomer, no solvent, at 190 °C, and high monomer/catalyst ratios). In fact, complexes **1**−**4**, bearing bidentate [N,O$^-$] ligands are less active under the former conditions with respect to complex **5**, bearing a tridentate [N,O$^-$,N] ligand, but they become much more active under the latter ones, rivaling with the performance of $Sn(Oct)_2$ tested under the same conditions. A kinetic study showed that the activation energy for **5** is significantly lower than that of complex **3** (chosen as a representative example of ligands bearing bidentate ligands). DFT calculations confirmed the role of the coordination of the additional pyridine moiety in decreasing the activation energy for the first insertion of the L-LA into the Zn-OR bond of the active species. Finally, preliminary depolymerization tests via methanolysis of commercial isotactic PLLA samples under mild conditions afforded methyl lactate with high activity and selectivity. Future work will address this interesting route to the chemical recycling of post-use PLA waste as well as a scale-up of the polymerization using larger reactors with more efficient mechanical stirring to target the production of polymers with higher molecular weights.

ASSOCIATED CONTENT

Supporting Information

The Supporting Information is available free of charge at https://pubs.acs.org/doi/10.1021/acs.macromol.2c00719.

Cartesian coordinates of DFT structures discussed in the text (XYZ)

X-ray crystallographic CIF for complex **4** (CIF)

Materials and methods, synthesis and characterization of complexes, NMR experiments, MALDI-ToF MS spectra, ^{1}H and ^{13}C NMR spectra, DSC thermograms, polymerization procedures, kinetic plots, details of DFT calculations, and X-ray diffraction (PDF)

X-ray crystallographic CIF for complex **2** (CIF)

AUTHOR INFORMATION

Corresponding Author

Claudio Pellecchia − *Dipartimento di Chimica e Biologia "A. Zambelli", Università di Salerno, Fisciano (SA) 84084, Italy;* orcid.org/0000-0003-4358-1776; Email: cpellecchia@unisa.it

Authors

Massimo Christian D'Alterio − *Dipartimento di Chimica e Biologia "A. Zambelli", Università di Salerno, Fisciano (SA) 84084, Italy;* orcid.org/0000-0003-0064-903X

Ilaria D'Auria − *Dipartimento di Chimica e Biologia "A. Zambelli", Università di Salerno, Fisciano (SA) 84084, Italy;* orcid.org/0000-0002-3561-012X

Licia Gaeta − *Dipartimento di Chimica e Biologia "A. Zambelli", Università di Salerno, Fisciano (SA) 84084, Italy*

Consiglia Tedesco − *Dipartimento di Chimica e Biologia "A. Zambelli", Università di Salerno, Fisciano (SA) 84084, Italy;* orcid.org/0000-0001-6849-798X

Stefano Brenna − *Dipartimento di Scienza e Alta Tecnologia, Università dell'Insubria, Como 22100, Italy;* orcid.org/0000-0002-2873-2436

Complete contact information is available at: https://pubs.acs.org/10.1021/acs.macromol.2c00719

Notes

The authors declare no competing financial interest.

ACKNOWLEDGMENTS

This research was funded by the University of Salerno (FARB). We thank Dr. Patrizia Iannece for MALDI-MS measurements. Dr. Barbara Immirzi and Dr. Giovanni Dal Poggetto, Istituto per

i Polimeri, Compositi e Biomateriali, CNR, Pozzuoli, are gratefully acknowledged for the SEC measurements.

REFERENCES

(1) Schneiderman, D. K.; Hillmyer, M. A. 50th Anniversary Perspective: There is a Great Future in Sustainable Polymers. *Macromolecules* **2017**, *50*, 3733−3749.
(2) Castro-Aguirre, E.; Iñiguez-Franco, F.; Samsudin, H.; Fang, X.; Auras, R. Poly(lactic acid)-Mass Production, Processing, Industrial Applications, and End of Life. *Adv. Drug Delivery Rev.* **2016**, *107*, 333−366.
(3) Haider, T. P.; Völker, C.; Kramm, J.; Landfester, K.; Wurm, F. R. Plastics of the Future? The Impact of Biodegradable Polymers on the Environment and on Society. *Angew. Chem., Int. Ed.* **2019**, *58*, 50−62.
(4) Zhang, X.; Fevre, M.; Jones, G. O.; Waymouth, R. M. Catalysis as an Enabling Science for Sustainable Polymers. *Chem. Rev.* **2018**, *118*, 839−885.
(5) McKeown, P.; Jones, M. D. The Chemical Recycling of PLA: A Review. *Sustain. Chem.* **2020**, *1*, 1−22.
(6) Coates, G. W.; Getzler, Y. D. Y. L. Chemical recycling to monomer for an ideal, circular polymer economy. *Nat. Rev. Mater.* **2020**, *5*, 501−516.
(7) Martin, R. T.; Camargo, L. P.; Miller, S. A. Marine-degradable polylactic acid. *Green Chem.* **2014**, *16*, 1768−1773.
(8) Kundys, A.; Plichta, A.; Florjańczyk, Z.; Zychewicz, A.; Lisowska, P.; Parzuchowski, P.; Wawrzyńska, E. Multi-arm star polymers of lactide obtained in melt in the presence of hyperbranched oligoglycerols. *Polym. Int.* **2016**, *65*, 927−937.
(9) Nakayama, Y.; Aihara, K.; Yamanishi, H.; Fukuoka, H.; Tanaka, R.; Cai, Z.; Shiono, T. Synthesis of Biodegradable Thermoplastic Elastomers from ε-Caprolactone and Lactide. *J. Polym. Sci., Part A: Polym. Chem.* **2015**, *53*, 489−495.
(10) Hillmyer, M. A.; Tolman, W. B. Aliphatic Polyester Block Polymers: Renewable, Degradable, and Sustainable. *Acc. Chem. Res.* **2014**, *47*, 2390−2396.
(11) Byers, J. A.; Biernesser, A. B.; Delle Chiaie, K. R.; Kaur, A.; Kehl, J. A. Catalytic systems for the production of Poly(lactic acid). *Adv. Polym. Sci.* **2017**, *279*, 67−118.
(12) Kowalski, A.; Duda, A.; Penczek, S. Mechanism of Cyclic Ester Polymerization Initiated with Tin(II) Octoate. 2. Macromolecules Fitted with Tin(II) Alkoxide Species Observed Directly in MALDI−TOF Spectra. *Macromolecules* **2000**, *33*, 689−695.
(13) Petrus, R.; Sobota, P. Magnesium and Zinc Alkoxides and Aryloxides Supported by Commercially Available Ligands as Promoters of Chemical Transformations of Lactic Acid Derivatives to Industrially Important Fine Chemicals. *Coord. Chem. Rev.* **2019**, *396*, 72−88.
(14) Kremer, A. B.; Mehrkhodavandi, P. Dinuclear Catalysts for the Ring Opening Polymerization of Lactide. *Coord. Chem. Rev.* **2019**, *380*, 35−57.
(15) Chamberlain, B. M.; Cheng, M.; Moore, D. R.; Ovitt, T. M.; Lobkovsky, E. B.; Coates, G. W. Polymerization of Lactide with Zinc and Magnesium β-Diiminate Complexes: Stereocontrol and Mechanism. *J. Am. Chem. Soc.* **2001**, *123*, 3229−3238.
(16) Rosen, T.; Goldberg, I.; Navarra, W.; Venditto, V.; Kol, M. Block-Stereoblock Copolymers of Poly(ε-Caprolactone) and Poly-(Lactic Acid). *Angew. Chem.* **2018**, *130*, 7309−7313.
(17) D'Auria, I.; Tedesco, C.; Mazzeo, M.; Pellecchia, C. New Homoleptic Bis(pyrrolylpyridiylimino) Mg(II) and Zn(II) Complexes as Catalysts for the Ring Opening Polymerization of Cyclic Esters via an Activated Monomer Mechanism. *Dalton Trans.* **2017**, *46*, 12217−12225.
(18) D'Auria, I.; D'Alterio, M. C.; Tedesco, C.; Pellecchia, C. Tailor-Made Block Copolymers of L-, D- and rac- Lactides and ε-Caprolactone via One-Pot Sequential Ring Opening Polymerization by Pyridylamidozinc(II) Catalysts. *RSC Adv.* **2019**, *9*, 32771−32779.
(19) Hermann, A.; Hill, S.; Metz, A.; Heck, J.; Hoffmann, A.; Hartmann, L.; Herres-Pawlis, S. Next Generation of Zinc Bisguanidine Polymerization Catalysts towards Highly Crystalline, Biodegradable Polyesters. *Angew. Chem., Int. Ed.* **2020**, *59*, 21778−21784.
(20) Rittinghaus, R. D.; Schäfer, P. M.; Albrecht, P.; Conrads, C.; Hoffmann, A.; Ksiazkiewicz, A. N.; Bienemann, O.; Pich, A.; Herres-Pawlis, S. New Kids in Lactide Polymerization: Highly Active and Robust Iron Guanidine Complexes as Superior Catalysts. *ChemSusChem* **2019**, *12*, 2161−2165.
(21) McKeown, P.; McCormick, S. N.; Mahon, M. F.; Jones, M. D. Highly Active Mg(II) and Zn(II) Complexes for the Ring Opening Polymerisation of Lactide. *Polym. Chem.* **2018**, *9*, 5339−5347.
(22) D'Auria, I.; Ferrara, V.; Tedesco, C.; Kretschmer, K.; Kempe, R.; Pellecchia, C. Guanidinate Zn(II) Complexes as Efficient Catalysts for Lactide Homo- and Copolymerization under Industrially Relevant Conditions. *ACS Appl. Polym. Mater.* **2021**, *3*, 4035−4043.
(23) Ardizzoia, G. A.; Colombo, G.; Therrien, B.; Brenna, S. Tuning the Fluorescence Emission and HOMO-LUMO Band Gapn in Homoleptic Zinc(II) Complexes with N,O-Bidentate (Imidazo[1,5-a]pyrid-3-yl)phenols. *Eur. J. Inorg. Chem.* **2019**, *2019*, 1825−1831.
(24) Gao, Q.; Chen, Y.; Liu, Y.; Li, C.; Gao, D.; Wu, B.; Li, H.; Li, Y.; Liu, W.; Li, W. A series of Zn(II) and Co(II) complexes based on 2-(imidazo[1,5-a]pyridin-3-yl)phenol: syntheses, structures, and luminescent and magnetic properties. *J. Coord. Chem.* **2014**, *67*, 1673−1692.
(25) Jędrzkiewicz, D.; Ejfler, J.; Gulia, L.; John, Ł.; Szafert, S. Designing ancillary ligands for heteroleptic/homoleptic zinc complex formation: synthesis, structures and application in ROP of lactides. *Dalton Trans.* **2015**, *44*, 13700−13715.
(26) D'Alterio, M. C.; De Rosa, C.; Talarico, G. Stereoselective Lactide Polymerization: the Challenge of Chiral Catalyst Recognition. *ACS Catal.* **2020**, *10*, 2221−2225.
(27) D'Alterio, M. C.; De Rosa, C.; Talarico, G. Syndiotactic PLA from meso-LA Polymerization at Al-Chiral complex: a probe of DFT mechanistic insights. *Chem. Commun.* **2021**, *57*, 1611−1614.
(28) Fliedel, C.; Vila-Viçosa, D.; Calhorda, M. J.; Dagorne, S.; Aviles, T. Dinuclear Zinc−N-Heterocyclic Carbene Complexes for Either the Controlled Ring-Opening Polymerization of Lactide or the Controlled Degradation of Polylactide Under Mild Conditions. *ChemCatChem* **2014**, *6*, 1481.
(29) Petrus, R.; Bykowski, D.; Sobota, P. Solvothermal Alcoholysis Routes for Recycling Polylactide Waste as Lactic Acid Esters. *ACS Catal.* **2016**, *6*, 5222−5235.
(30) Román-Ramírez, L. A.; McKeown, P.; Jones, M. D.; Wood, J. Poly(lactic acid) Degradation into Methyl Lactate Catalyzed by a Well-Defined Zn(II) Complex. *ACS Catal.* **2019**, *9*, 409−416.
(31) Santulli, F.; Lamberti, M.; Mazzeo, M. A Single Catalyst for Promoting Reverse Processes: Synthesis and Chemical Degradation of Polylactide. *ChemSusChem* **2021**, *14*, 5470−5475.

https://doi.org/10.1021/acs.macromol.2c00719
Macromolecules 2022, 55, 5115−5122